Military Technical College
Kobry El-Kobbah,
Cairo, Egypt.

17th International Conference on Applied Mechanics and Mechanical Engineering.

AUTOMATED INSPECTION OF SURFACE DEFECTS USING MACHINE VISION

M. El-Agamy [*], M. A. Awad [†] and H. A. Sonbol [‡]

ABSTRACT

Surface defects represent a major threat for product quality and its function that require proper inspection. Variety of surface defects makes their inspection more complicated, costly and requires longer time. Reliance on human inspection can lead also to less consistent results due to the variance in expertise and human error. For those reasons, traditional inspection methods less fit to fast automated manufacturing systems. Employing computer vision techniques in vision –based Inspection systems (VBI) can lead to developing better systems that match modern manufacturing systems in terms of speed, automation, higher productivity, less dependency human experience and cost optimization. In this research, an automated vison-based inspection system (CAI-2) is developed for detection and classification of surface defects encountered in metal parts using Digital Image Processing (DIP) techniques. CAI-2 receives the image of the part under inspection as an input, detects and generates automatically the type, number and location of existing surface defects. Six types of surface can be detected using the proposed method including Cracks, dents, fretting, flaking, rust, and smearing. The accuracy and effectiveness of the developed model were evaluated against skilled inspectors by measuring the values of inspection time, recall, precision and f-measure parameters values. Experimental results proved competitive accuracy and efficiency of the proposed inspection model compared to traditional inspection methods.

KEYWORDS

Artificial Neural Networks, Computer Vision, Digital Image Processing, Visual-Based Inspection.

[*] Col. Eng., Master Degree in Mechanical Engineering /elagamy_2000@yahoo.com.
[†] Ass. Professor, Design and Prod, Eng. Dpt., Ain Shams University, Cairo, Egypt.
[‡] Professor, Design and Prod, Eng. Dpt., Ain Shams University, Cairo, Egypt.

INTRODUCTION

Surface defects impact product surface quality and its function. Surface defects include Cracks, Smearing, Corrosion, Dents and Flaking as shown in Fig.1.b. Crack is a fracture passing through grain boundaries that result from overstressing which may occur during forging, forming or during heat treatment operations. Corrosion is an interaction between metal surface and its environment that results in negative impacts on material and products mechanical properties and function. Dent is a depression in surface results of a pressure or impact force. Flaking is a fatigue effect that occur when the part reaches its end of its normal life span, exposure to excessive load or as a result of indentations, rust or smearing. Smearing is material transfer between two in-contact sliding surfaces under excessive load and/or improper lubrication [7].

Surface inspection methods involve two main methods: Traditional (manual) inspection methods performed with expertise inspectors and machines assisted / or automated inspection methods. Traditional inspection methods of surface defects are mainly dependent on human experience using visual inspection methods. Compared with automated methods, Manual inspection methods consume longer time, effort, may provide inconsistent results, subjective to inspector judgment, hence they are inappropriate for high speed automated manufacturing systems.

Computer vision has contributed in development of vision-based inspection systems (VBIs) using image processing techniques [1-3]. VBIs applications increased in manufacturing industry because they support automation, consistency, standardization, integration and higher productivity while decreasing the inspection cost, time and required inspection skills. Traditional inspection systems are expensive in time, effort and unreliable in mass production and high speed automated systems, as acceptance decision is more dependent on human perception and experience [4-6].

Using VBIs in detection and classifications of surface defects requires using proper image processing techniques to handle noises in part images that can result from variance in illuminations or part surface roughness especially metal parts. Traditional inspection methods of surface defects are mainly dependent on human experience using visual inspection methods. Manual inspection results are highly dependent on inspector expertise and accuracy, which does not guarantee of final product quality besides their high cost and longer times. Therefore, VBIs are more efficient in surface defects inspection in modern automated manufacturing systems.

This research introduces new VBI for automated detection and classification of metal surface defects using pattern matching technique. Classification of surface defects requires having suitable defect images database that cover required defect types. Therefore, the required setup was prepared and images of defected parts were captured. Image preparation and enhancement technique are used to prepare and improve image quality. Then, the proposed algorithm is applied for searching, detection and classification of surface defects using pattern matching technique. Finally, system capability was assessed against manual inspection method to verify its capability.

LITERATURE REVIEW

Computer vision has been proposed in many research works for VBIs in different industries. Schmitt et al. [8] proposed an inline inspection system for carbide tool inserts coating and geometry. The accuracy of the system was high, yet applicable for special type of tool inserts [8]. VBIs were developed also for detection of defects in fabric [9] and textile using Gray level co-occurrence matrix to extract the flaws features in fabric and texture images, and then BPANN for their classifications of fabric. Experimental results showed an accuracy of this system of 97.14% [10].

However, both researches had poor accuracy at low contrast surfaces. VBIs were proposed also for extracting and classification of wood sheets defects. Pham and Alcock [11] method detected 32 defect types and used ANNs for classification. Regardless number of detected defects types, the developed method was applicable for Veneer wood boards only and no comparison made with human inspection method to assess its effectiveness [11].

Another approach was used to detect and classify defects in aluminum foil using convex hulls and brightness to detect bolt, fracture, scratch and spot defects. However, the study had similar limitations work in terms of the applicability and number of detected defects [12]. Kuo et al. [13] used similar VBI System for defect detection in LCD filters including: fiber, particle, gel, and resist coating. The Defect feature including defect area, aspect ratio, squareness ratio and damage ratio are calculated and input to BPNN to classify the defects. Although the mentioned that accuracy was 94% and reduction of production costs [13] however, there is no explanation how these ratios were automatically calculated.

Jahanshahi et al. [14] proposed a remote crack detection system for structural parts. Image processing and MLP ANNs were used in classification of detected cracks. The developed system can detect cracks with 0.1 mm thickness from a distance of 20 meters. However, the accuracy of crack detection was highly affected by incident light.

Sills et al. [15] developed an algorithm to identify surface porosities, dents and scratches via illuminating machined surfaces. A reflection model for each point in imaged surface is developed. A surface defect is detected when difference exist between observed reflected incident lighting angle and the developed reflection model. The limitation of this method is its slow processing and ignorance of surface roughness variance, which limits applicability of the developed system to different surfaces. Qinghua et al. [16] developed a VBI for inspection of tapered roller bearing, but it did not include the bearing shield inspection.

Deng et al. [17] designed another method for bearing surfaces inspection but did not mention how to inspect logos on the bearing seal. Shen et al. [5] developed another VBI system for inspection of bearing covers defects including deformations, rusts, and scratches. They compared the inspection results with the human traditional inspection methods. The findings show close accuracy to human inspection methods.

However, they focused only of deformation of bearing covers and did not address how other defects can be detected [5]. To sum up, the presented VBI methods have the following limitations: (1) little research works examined combined defects in the same

part; (2) few number of detected defects during production like cracks or defects only; (3) limited applicability of developed methods to specific applications; (4) little research on inspection of metal parts; (5) most inspection methods are developed for in process inspection only; (6) lack of creditability of the proposed methods because no benchmarking was made against human inspection methods.

RESEARCH AIM AND OBJECTIVES

The aim of this research is to develop an automated VBI system for detection and classification of surface defects in metal parts. The main objectives are: first, developing VBI that can detect and classify common surface defects encountered in manufactured parts; secondly, verifying system capability against traditional inspection methods.

METHODOLOGY

CAI-2 model is structured from two main modules: image enhancement module and defect detection module. The main steps of the proposed models and samples of the detected defects are shown in Fig.1. The program was written developed using Matlab and LabView software.

Setup and Image Acquisition

The setup of the developed inspection system includes Area Scan CCD camera, lenses, ring-shaped white light LED illuminator, light shield, laptop and motor-driven conveyor. The camera is triggered with resolution factor of 1600*1200, part under inspection are placed on the conveyor, facing the camera and lenses. Illumination is adjusted and light shield is used to reduce surrounding light noises effects in the acquired images. Images are calibrated to interpret measurement from pixels into real-world units (mm) for convenience where the distance between two selected pixels, are used as a reference. Then, images are converted from colored Image to grey scale images (from RGB into HSI space) as shown in Fig.4a to facilitate their further analysis.

CAI-2 uses pattern matching technique to inspect the examined surface images and to detect the level of matching with stored defects templates in the program database. The program database was developed using 300 images of different types of surface defects in manufactured parts. Defect types included cracks, dents, corrosion, flaking, fretting, rust, and smearing.

Image Enhancement

Captured images normally have variation in contrast and brightness due to camera sensitivity, variance in surface roughness and illumination noise [18]. Image enhancement is applied on the image spatial domain to enhance image quality,

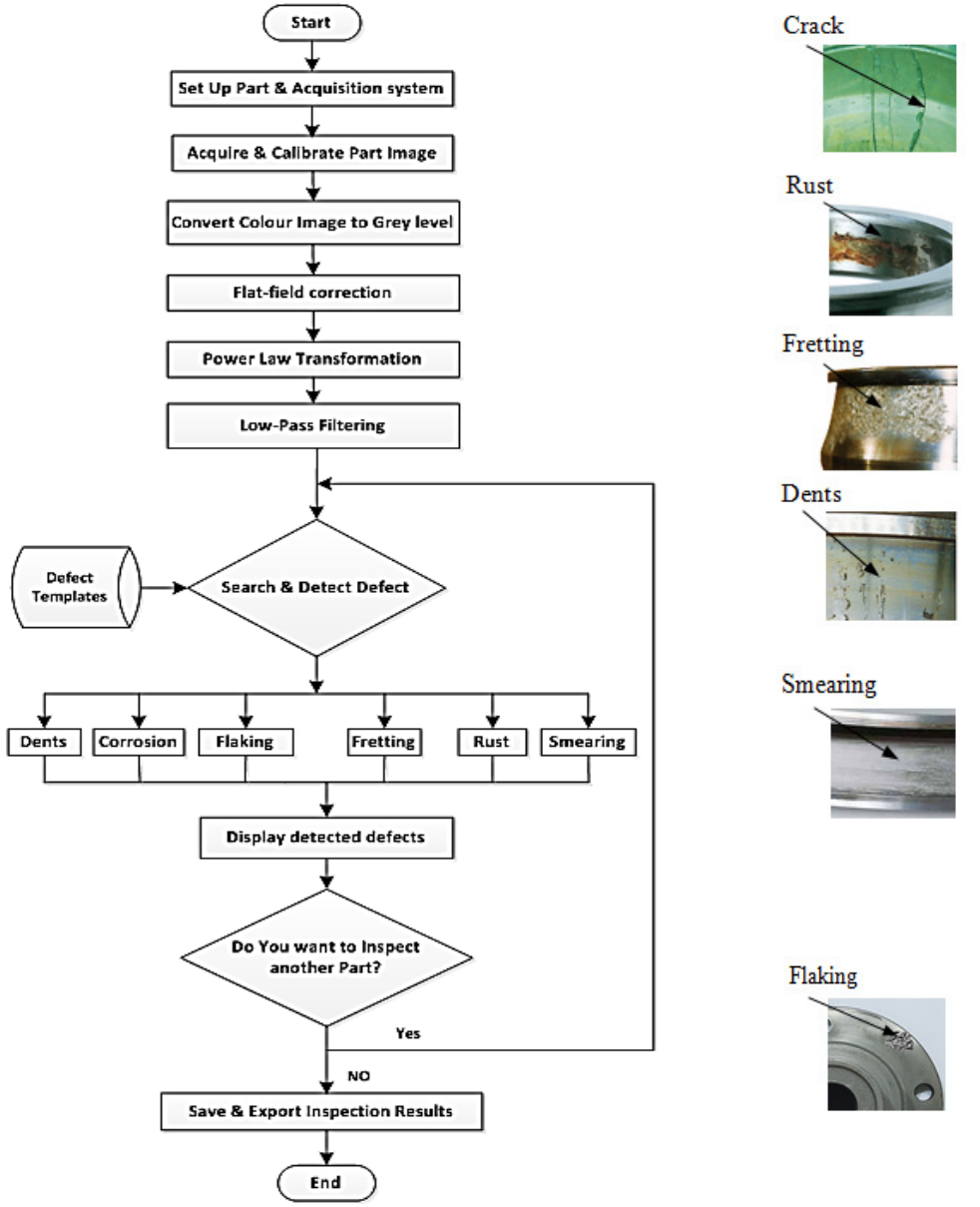

a. CAI-2 Process Flow Model b. Surface Defects

Fig.1. CAI-2 Inspection Model for surface defects.

minimize existing noise and ensure that all images have the same range of contrast and brightness. Accordingly, existing defect features can be distinguishable and extracted from other surface textures [19]. In this work, image enhancement encompasses two main steps: Flat Field Correction and Power-Law Transformation

Flat field correction is applied on the captured images to correct illumination variance in captured images as shown in Fig.4b. This occurs due to camera lens vignetting (higher concentration of brightness at image center region than its periphery), non-linearity of examined surface roughness, sensor sensitivity and dust and impurity effects in the light path between camera lens and the examined part. CCD camera chips are not evenly sensitive to light at specific wavelengths across their entire range

because of noise that interferes with photons and prevents them from getting to the correct location on the chip [100]. Bright and dark field background images are captured during system setup and used in correction of image brightness correction using the formula (2). However, resultant image after flat field correction has relatively poor contrast between grey levels as shown in Fig. 4c. . So, Power-law transformation is used.

Power-Law transformation produces clear and more detailed images grey levels as shown in in Fig. 4d.it increases the grey level values in dark image regions when using γ < 1; and does the opposite for white images when using γ >1. In this work, γ values are selected (0.4; 1.5). The aim is to generate brighter images with more details while not affecting the surface texture under inspection. The formula used in power-law transformation is calculated by equation (1).

$$S = cr^{\gamma} \qquad (1)$$

where S and r are the output and input image grey levels; c and γ are constants.

Pattern Search and Matching

After image enhancement, images are scanned to detect similar defect pattern to those stored in the developed defect database. The location, angle and % match (maximum correlation value) of the detected pattern are determined using normalized correlation algorithm. This algorithm is used for training and testing the CAI-2 system. The average brightness of image is subtracted from the grey level value of each pixel in both the reference defect template and the part image which eliminates the difference in the brightness. The best match is determined when the highest correlation is reached and defect pattern is detected. Using this algorithm provides stable pattern results because it is not affected by light conditions between defect template and part image. However, this process is a time consuming depending on image size. So, image sampling is performed to avoid this limitation.

The image size is reduced by applying image sampling to reduce the number of scanned pixels and the volume of data being processed. Low pass filtering using Gaussian Pyramid Decomposition is used for reducing the input images size to one-fourth of their original sizes. Suitable number of GPD levels is selected to balance between speed and accuracy of the matching process. The GPD code was developed using Matlab software.

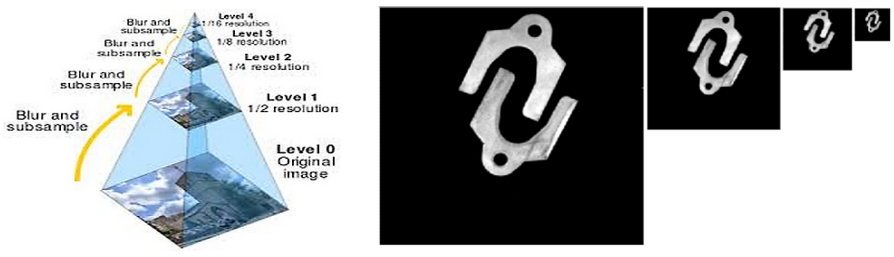

Fig. 2. Image Resampling using Gaussian Pyramid Decomposition.

Figure 3 illustrates the search and matching procedure using the normalized cross correlation algorithm. The process involves moving the template or sub-image w over the image area and to find the best match location. The process encompasses multiplying template pixels that overlaps and then summing the results over all the pixels of the template. The normalized correlation coefficient is used, which is calculated by equation (2):

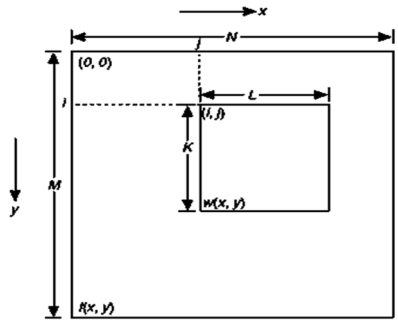

(a) Search Layout

$$R(i,j) = \frac{\sum_{x=0}^{L-1}\sum_{y=0}^{K-1}(w(x,y)-\bar{w})(f(x+i,y+j)-\bar{f}(i,j))}{\left[\sum_{x=0}^{L-1}\sum_{y=0}^{K-1}(w(x,y)-\bar{w})^2\right]^{\frac{1}{2}}\left[\sum_{x=0}^{L-1}\sum_{y=0}^{K-1}(f(x+i,y+j)-\bar{f}(i,j))^2\right]^{\frac{1}{2}}} \quad (2)$$

(b) Normalized Cross correlation algorithm

Fig.3. Correlation search and algorithm.

where $\bar{w}$ is the average intensity value of the pixels in the template w. The variable $\bar{f}$ is the average value off in the region coincident with the current location of w. The value of R lies in the range –1 to 1 and is independent of scale changes in the intensity values of f and w.

CAI-2 model was trained using the images stored in the created database. During training, the model learns and stores the gray level and edge gradient values in the provided defect template. Then, it proceeds and computes the optimum pyramid level that can be utilized for each given template and learns the information required to characterize those templates in different possible rotated forms at different levels. During the matching process, the model examines the inspected images, and detects the best match according to the highest cross-correlation value. CAI-2 detects the type, number and location of surface defects with their matching score as shown in Fig. 4e. The higher the matching score, the higher matching with the stored defect template.

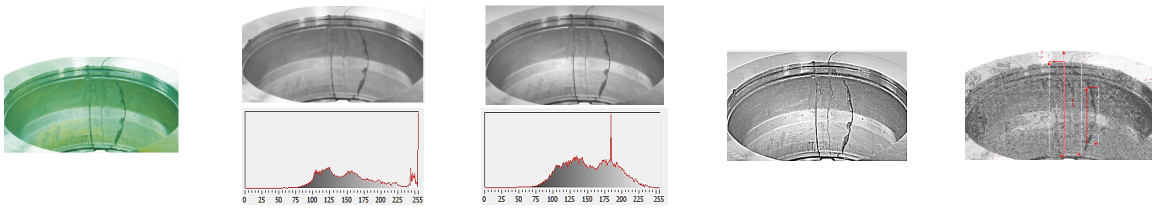

a. Acqiured Image | b. Grey Level Image | c. Flat-Field Correction | d. Power-Law Transf. | e. 3 Detected Defects

Fig. 4. Image Enhanceemnt Steps.

VERIFICATION OF MODEL CAPABILITIES

The developed model was tested to determine its accuracy by comparing its capabilities against experienced inspectors. A sample of 960 parts images was collected and classified into 6 groups representing the examined defects types: Cracks, dents, fretting, rust, flaking, and smearing. Inspected parts include inner and outer bearings races, flanges and gears. The sample included 731 good parts and 229 defected parts. All samples are collected by experienced inspectors and inspected carefully by 3 expertise inspectors, where their final judgment is considered the ground truth for this test. System capability is benchmarked against human inspectors as illustrated in Table 1.

Evaluation Criteria

In this research, the values of the recall, precision and F-measure are calculated and used to evaluate the model accuracy. Precision is the inspection results that are true positives calculated as percentage of the correctly detected good parts to the whole detected good parts. Recall represents the true positives, calculated as the ratio of correct detected good parts to the whole ‘‘ground truth’’ good parts and calculated by the following equations:

$$Precision = \frac{TP}{TP + FP} * 100\% \quad (3)$$

$$Recall = \frac{TP}{TP + FN} * 100\% \quad (4)$$

where TP is the correct accepted good parts, FN is the defective parts that are incorrectly accepted as good ones, and FP is the good parts that are incorrectly accepted as defective ones.

The F-measure is the weighted harmonic average of precision and recall, calculated by equation (5):

$$\mathrm{F}\,\alpha = \frac{(1+\propto) * Precision * Recall}{\propto * Precision + Recall} \quad (5)$$

where $\propto$ is a positive real value of the weighted coefficient between recall and precision $\propto$ is selected = 0.8 in this work to weigh recall more than precision.

Results

Defect inspection results of CAI-2 vs. Human Inspectors are presented in Appendix (B). Defect detection accuracy evaluation in terms of selected criteria: Recall, Precision and Fα are charted. The calculated F-measure of each sample for CAI-2 for defect detection is relatively high for: Dents (94.58), Fretting (93.97), Rust (95.00), Fatigue (95.59), Indentations (95.84) and Smearing (95.84); while it was relatively lower for in Cracks (91.62).

Table 1. CAI-2 vs. Human Inspectors Capabilities.

Method	Selected Range	Crack	Dent	Fretting	Rust	Flaking	Smearing
CAI-2	Length (mm)	2	0.1	2	2	2	3
H. Insp.		2	0.1	2	2	2	3
CAI-2	Width / Thickness (mm)	0.2	0.1	2	2	2	3
H. Insp.		0.2	0.1	2	2	2	3
CAI-2	Angle (Deg.)	0:360	0:360	0:360	0:360	0:360	0:360
H. Insp.		0:360	0:360	0:360	0:360	0:360	0:360
CAI-2	Recall %	89.5	94.1	91.8	95.0	93.8	96.5
H. Insp.		94.8	95.2	94.9	95.2	94.1	94.5
CAI-2	Precision %	93.4	95.0	95.7	95.0	93.8	95.3
H. Insp.		100	100	100	100	100	100
CAI-2	Fα %	91.6	97.6	94.0	95.0	93.8	95.8
H. Insp.		97.6	94.6	97.7	97.8	97.3	97.5

There are no good parts classified as a bad ones by inspectors because each is expertise and shall inspect each defective part carefully for several times. Meanwhile, acceptance criterion was selected according to expert acceptance. This justifies higher final calculated F-measure values related to human inspectors compared with those of CAI-2. The maximum difference in recall value between CAI-2 and the inspector was 7 % maximum, which indicates the high accuracy of CAI-2. Most of the wrong recognitions are detected in samples that has high variance in illumination or that have surface features that vary in levels, which in turn require masking those feature regions in the acquired image to avoid faulty identified defects that not actually exist.

CASE STUDY

This case study illustrates implementation of CAI-2 for general parts. CAI-2 receives the part image as an input, then proceeds to image processing including image transformation, resizing and enhancement. Finally, the model proceeds to searching for, detection, classification and generating the existing type, number, location of existing defects with inspection time. The model was simulated using a test sample of 7 different parts shown in Appendix (A) with various sizes and features verify its generalization capabilities.

CAI-2 could generate the type, locations, and number and inspection times. To compare the inspection time required by CAI-2 with human inspectors, Each part was inspected three times by three different inspectors in random order and the average total inspection time required for all parts was calculated (T1).

The inspection cycle using CAI-2 was repeated three times for the same parts and the average total time (T2) was calculated too. By comparing both inspection times, the result shows that T2 is less than 10% T1 for dents, cracks, and was less than 20% T1 for other defect types. The results show successful implementation of CAI-2 model in the defect. The average time for defects inspection by CAI-2 was 1.75 s. including image acquisition time (0.5 s), the total time was less than 1.75 s. So CAI-2 can be considered suitable for speed automated manufacturing system for its time and the accuracy that found competitive to human inspectors. Accordingly, CAI-2 can be used

as used as a substitute of human inspection or integrated to enhance and increased the creditability of inspection results.

CONCLUSION AND FUTURE WORK

In this research, new automated vision based-system was presented for detection of different surface defects. CAI-2 employs computer vision techniques in defect identification and characterization. The system can detect, classify and count the surface defects including Cracks, dents, fretting, flaking, fatigue and smearing. The developed model meets the requirements modern automated manufacturing systems and can be adopted and developed for integration with machine vision systems. It is flexible to use; can detect six types of surface defects; able to detect combination of defects in same part; developed for general applications-not for neither specific parts nor applications-; has a higher speed and competitive accuracy against human inspection methods. The efficiency of CAI-2 model can be enhanced via integration with artificial intelligence technologies like ANNs development of intelligent inspection decision systems. Using the ANN can enhance the CAI-2 capability to deal with more complicated inputs.

REFERENCES

[1] Turek, F. “Machine Vision Fundamentals: How to Make Robots”, NASA Tech Briefs Magazine, 2011, Vol. 35. pp. 60–62.

[2] Abouelatta, O.B., “3D Surface Roughness Measurement Using a Light Sectioning Vision System”, Proceedings of the World Congress on Engineering, 2010,Vol. I, pp.698–703.

[3] Steger, C., Markus, U., and Christian W. (ed) Machine Vision Algorithms and Applications. Weinheim New York, 2008, p. 1.

[4] Deák, K. Kocsis, I. Vámosi, A. (2014) “Application of machine vision in manufacturing of bearings using ANN and SVM” Proceedings of the 9th Int. Conf. on Applied Informatics Eger, Hungary, January 29–February 1, 2014. Vol. 1. pp. 295–304 doi: 10.14794/ICAI.9.2014.1.295

[5] Shen, H. Li, S. Gu, D. Chang, H. (2012) Bearing defect inspection based on machine vision, Measurement,45, pp.719–733.

[6] Henry Y.Y. Ngan, Grantham K.H. Pang, Nelson H.C. Yung, Automated fabric defect detection – a review, Image Vis. Comput. 29 (2011) pp.442–458.

[7] Lipson, C. & Colwell, C. Handbook of mechanical wear: wear, frettage, pitting, cavitation, corrosion; University of Michigan Press, 1961; p. 449.

[8] Schmitt, R., Scholl, I., Cai1, Y., “Machine Vision System for Inline Inspection in Carbide Insert Production”, Proceedings of the 36th International MATADOR Conference, 2010.

[9] D. Martin, D.M. Guinea, M.C. Garcia-Alegre, E. Villanueva, D. Guinea,Multi-modal defect detection of residual oxide scale on a cold stainless steel strip, Mach. Vis. Appl. 21 (2010) pp.653–666.

[10] Su, T. and Lu, C. (2009) “Automated vision system for recognizing lycra spandex defects”. Retrieved from: www.fibtex.lodz.pl/2011/1/43.pdf

[11] Pham, D.T. and Alcock, R.J. (2009) Automated visual inspection of wood boards: selection of features for defect classification by a neural network, Proc Instn Mech Engrs Vol 213 Part E, pp.231-245.

[12] Lin, S., Chou, S. & Chen, S. (2007) "Irregular shapes classification by back-propagation neural networks", Int. J. of Adv. Manuf. Tech., Vol.34, pp.1164–1172.

[13] Kuo, C. Hsu, C. Fang,C. , Chao, S. & Lin, Y. (2012) "Automatic defect inspection system of colour filters using Taguchi-based neural network", Int. J. of Production Research.

[14] Jahanshahi, M.R., ·Masri, S. F., Padgett & C. W. (2013) "Sukhatme, G.S. An innovative methodology for detection and quantification of cracks through incorporation of depth perception, Machine Vision & Applications, pp.227–241.

[15] Sills, K. · Bone, G. M. & Capson, D. (2014) Defect identification on specular machined surfaces Machine Vision and Applications, 25:377–388. DOI 10.1007/s00138-013-0590-1

[16] Qinghua,W., Xunzhi, L. Zhen, Z. & Tao, H. (2010) "Defects inspecting system for tapered roller bearings based on machine vision", in: International Conf. on Electrical and Control Engineering, pp. 667–670.

[17] Deng, S., Cai, W. Xu, Q. & Liang, B.(2010) "Defect detection of bearing surfaces based on machine vision technique", Int. Conf. on Computer Application & System Modeling, pp. 548–554.

[18] Casado,C. O. (2010) "Image Contrast Enhancement Methods", Technical University – Sofia. From: http://academica-e.unavarra.es/xmlui/bitstream/handle/2454/2368/577327.pdf?sequence=1&isAllowed=y

[19] Khaled,A., Atia,, M.& Moussa, T. (2014) "Grey Cast Iron Categorization using Artificial Neural Network", International Journal of Scientific & Engineering Research, Volume 5, Issue 3, ISSN 2229-5518

Appendix (A). Implementation of CAI-2 in detection of surface Defects.

	Part 1	Part 2	Part 3	Part 4	Part 5	Part 6	Part 7
Acquistion	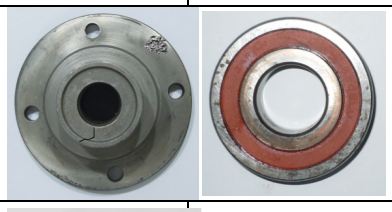		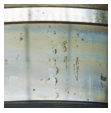			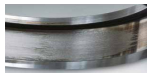	
Convert to grey image	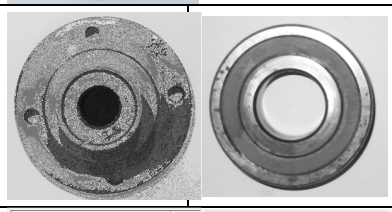		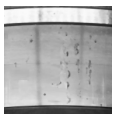			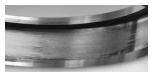	
	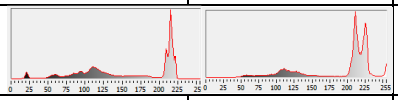		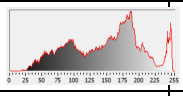	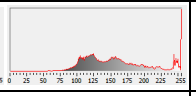	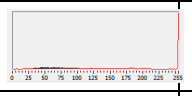	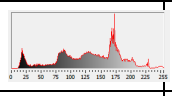	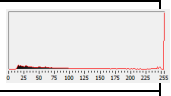
Flat field correction	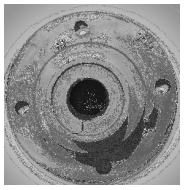		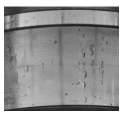	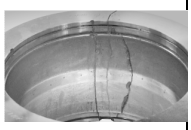		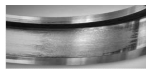	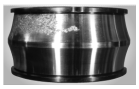
	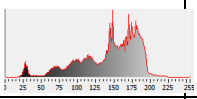	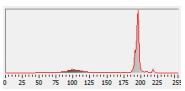	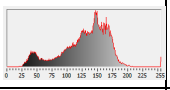	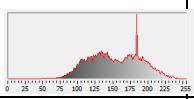	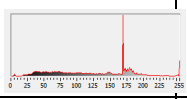	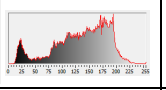	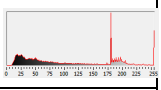
Power law Transform.			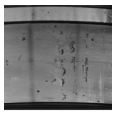	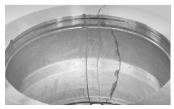			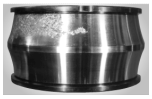
Lowpass filtering	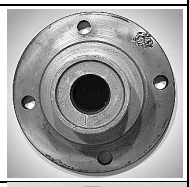						
Defect deetction							
Detected Defects	**Flaking & Crack**	**Rust**	**Dents**	**Cracks**	**Rust**	**Smearing**	**Fretting**

Appendix (B). Defect Inspection Results (CAI-2 vs. Human Inspectors).

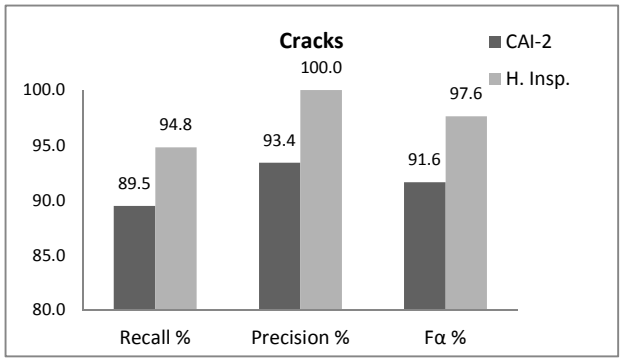

Fig. B.1

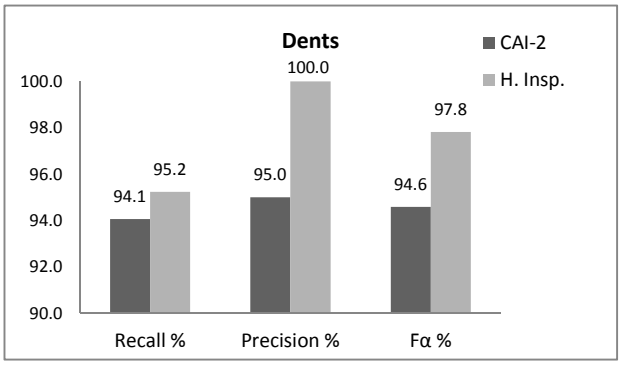

Fig. B.2

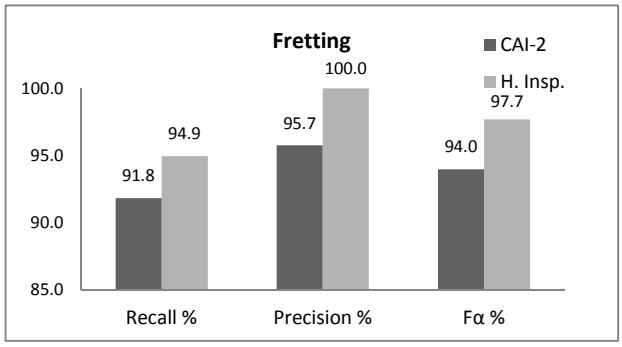

Fig. B.3

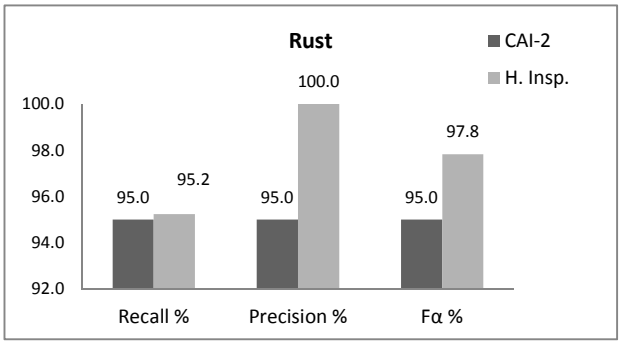

Fig. B.4

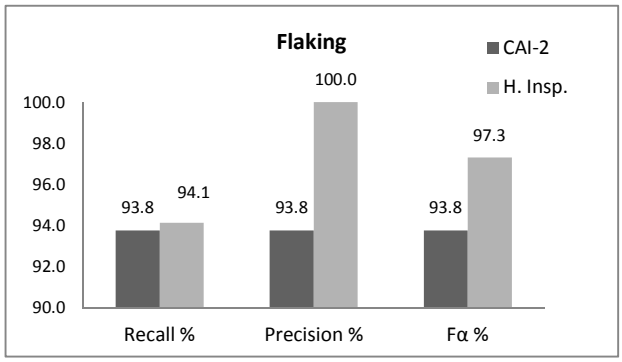

Fig. B.5

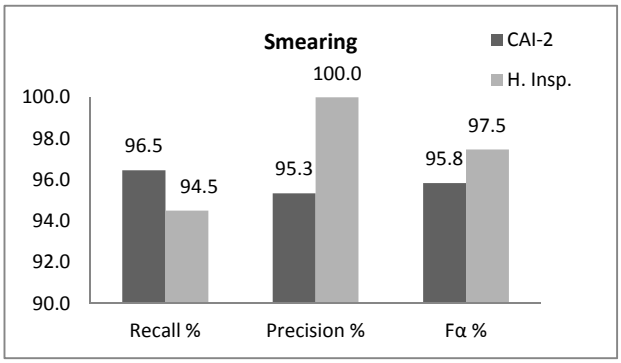

Fig. B.6